Editors' Suggestion | Featured in Physics

# Measurement of the Electrical Properties of a Thundercloud Through Muon Imaging by the GRAPES-3 Experiment

B. Hariharan,[1,2] A. Chandra,[1,2] S. R. Dugad,[1,2] S. K. Gupta,[1,2,*] P. Jagadeesan,[1,2] A. Jain,[1,2] P. K. Mohanty,[1,2] S. D. Morris,[1,2] P. K. Nayak,[1,2] P. S. Rakshe,[1,2] K. Ramesh,[1,2] B. S. Rao,[1,2] L. V. Reddy,[1,2] M. Zuberi,[1,2] Y. Hayashi,[2,3] S. Kawakami,[2,3] S. Ahmad,[2,4] H. Kojima,[2,5] A. Oshima,[2,5] S. Shibata,[2,5] Y. Muraki,[2,6] and K. Tanaka[2,7]

(GRAPES-3 Collaboration)

[1]*Tata Institute of Fundamental Research, Homi Bhabha Road, Mumbai 400005, India*
[2]*Cosmic Ray Laboratory, Raj Bhavan, Ooty 643001, India*
[3]*Graduate School of Science, Osaka City University, Osaka 558-8585, Japan*
[4]*Aligarh Muslim University, Aligarh 202002, India*
[5]*College of Engineering, Chubu University, Kasugai, Aichi 487-8501, Japan*
[6]*Institute for Space-Earth Environmental Research, Nagoya University, Nagoya, Aichi 446-8601, Japan*
[7]*Graduate School of Information Sciences, Hiroshima City University, Hiroshima 731-3194, Japan*

(Received 6 January 2019; revised manuscript received 21 January 2019; published 15 March 2019)

The GRAPES-3 muon telescope located in Ooty, India records rapid (∼10 min) variations in the muon intensity during major thunderstorms. Out of a total of 184 thunderstorms recorded during the interval of April 2011–December 2014, the one on December 1, 2014 produced a massive potential of 1.3 GV. The electric field measured by four well-separated (up to 6 km) monitors on the ground was used to help estimate some of the properties of this thundercloud, including its altitude and area that were found to be 11.4 km above mean sea level and $\geq 380$ km$^2$, respectively. A charging time of 6 min to reach 1.3 GV implied the delivery of a power of $\geq 2$ GW by this thundercloud that was moving at a speed of $\sim 60$ km h$^{-1}$. This work possibly provides the first direct evidence for the generation of gigavolt potentials in thunderclouds that could also possibly explain the production of highest-energy (100 MeV) gamma rays in the terrestrial gamma-ray flashes.

DOI: 10.1103/PhysRevLett.122.105101

Thunderstorms are a spectacular manifestation of the discharge of massive electric potentials that develop in thunderclouds during severe weather conditions. The first authoritative study of thunderstorms by Franklin dates back to the 1750s [1]. A major advance in their understanding occurred in the 1920s when their dipole structure was identified [2]. However, actual structure is more complex. The separation of electric charges in thunderclouds occurs when supercooled water droplets make grazing contact with hail pellets (graupel) polarized by the fine-weather electric field (120 V m$^{-1}$) on Earth's surface. The rebounding droplets acquire a positive charge and are carried by a convective updraft toward the cloud top, whereas negatively charged graupel fall toward the cloud base due to gravity. This creates a vertical field that increases the polarizing charge on the graupel, thus accelerating this process and reinforcing the vertical field that grows exponentially until air insulation breaks down and triggers a lightning discharge [3]. Because the thickness of thunderclouds extends to several kilometers, potentials of $\geq 1$ GV could be generated [2].

A unique signature of massive electric potentials generated in thunderclouds was the discovery of terrestrial gamma-ray flashes (TGFs) containing MeV photons by the BATSE instrument aboard the Compton Gamma Ray Observatory. The source of the TGFs was identified to be thunderstorms in the lower tropical atmosphere [4]. The detection of highest gamma-ray energy of 100 MeV by the AGILE satellite would, however, require bremsstrahlung of very high-energy electrons and the presence of potentials of hundreds of megavolts [5]. The maximum thunderstorm potential measured in balloon soundings is only 0.13 GV [6], which is well short of the magnitude needed to produce 100 MeV gamma rays [5] and the magnitude of 1 GV predicted by Wilson [2]. MeV gamma rays produced in thunderstorms have been detected on the ground, both through triggered and natural lightning discharges, showing a close connection of the TGFs detected from space and from the ground [7,8]. Early studies of the changes in muon intensity $I_\mu$ at low energies (90 MeV) were shown to be correlated with the electric field of thunderstorms [9,10] and confirmed by the results from Norikura [11] and elsewhere [12].

 

The Gamma Ray Astronomy at PeV EnergieS Phase-3 (GRAPES-3) muon telescope (G3MT) in Ooty [11.4°N, 2200 m above mean sea level (amsl)] studies the astrophysics of cosmic rays (CRs) through the measurement of $I_\mu$ produced by CRs. Its detection element is a proportional counter (PRC) made from steel pipes (6 m × 0.1 m × 0.1 m). The G3MT consists of four PRC layers under a 2 m thick concrete roof, resulting in a threshold of $E_\mu = 1\ \sec(\theta)$ GeV for muons with a zenith angle of $\theta$. This four-layer configuration enables muon reconstruction in two mutually perpendicular planes, and the two PRC layers in the same projection plane separated by ∼50 cm permit the muon direction to be measured with ∼4° accuracy, as shown in Fig. 1(a). Thus, the G3MT measures $I_\mu$ in 169 directions over a field of view; hereafter, FOV = 2.3 sr, as shown in Fig. 1(b) [13]. Although, the solid angle of 169 directions differ significantly, but the area of thundercloud covered varies by only 19%. Because $\sim 2.5 \times 10^6$ muons are recorded every minute, $I_\mu$ gets measured to 0.1% precision [14,15].

During thunderstorms, the G3MT detects rapid changes (∼10 min) in $I_\mu$. Because the muon energies exceed 1 GeV, the presence of large electric potentials is implied. To probe this phenomenon, electric field monitors, hereafter referred to as "EFMs" (Boltek model EFM-100 [16]), were installed in April 2011 at four locations: at GRAPES-3 and at three others a few kilometers away, as shown in Fig. 1(c). The data collected during April 2011–December 2014 showed that 184 thunderstorms were detected both by the G3MT and EFMs. The seven largest events with a muon intensity variation of $\Delta I_\mu \geq 0.4\%$ were shortlisted. However, except for the event on December 1, 2014 discussed here, the EFM profiles of the remaining six events were extremely complex, which made the association of $\Delta I_\mu$ and the electric field of a specific thundercloud difficult.

Thunderclouds are known to have a complex multipolar structure [3]; but here, it is assumed to be dipolar because the implications of such a structure can be easily simulated and a quantitative comparison of the simulation output with experimental data could be used to obtain the average properties of the thundercloud by treating it as a parallel plate capacitor that can provide an approximate estimate of its properties. To simulate the muon response to thundercloud potential $\mathbf{V}$, a uniform vertical electric field $\mathbf{E}_i$ for the following three cloud thickness cases $\mathbf{D}_i$ was investigated, where $\mathbf{V} = \mathbf{E}_i\mathbf{D}_i$: (1) $\mathbf{D}_1 = 2$ km for the field between 8 and 10 km amsl, (2) $\mathbf{D}_2 = 7.8$ km for the field between the ground and 10 km amsl, and (3) $\mathbf{D}_3 = 10$ km for the field between 10 and 20 km amsl. The dependence of $\Delta I_\mu$ on $\mathbf{V}$ was obtained from Monte Carlo simulations, which are described in the next paragraph and found to be the same for cases (1) and (2). For case (3), $\Delta I_\mu$ was 15% smaller than cases (1) and (2). Thus, case (3), apart from being unrealistic, also required potentials higher than the other two cases. Thus, a uniform electric field applied between 8 and 10 km was used to provide a conservative estimate of the thundercloud potential $\mathbf{V}$.

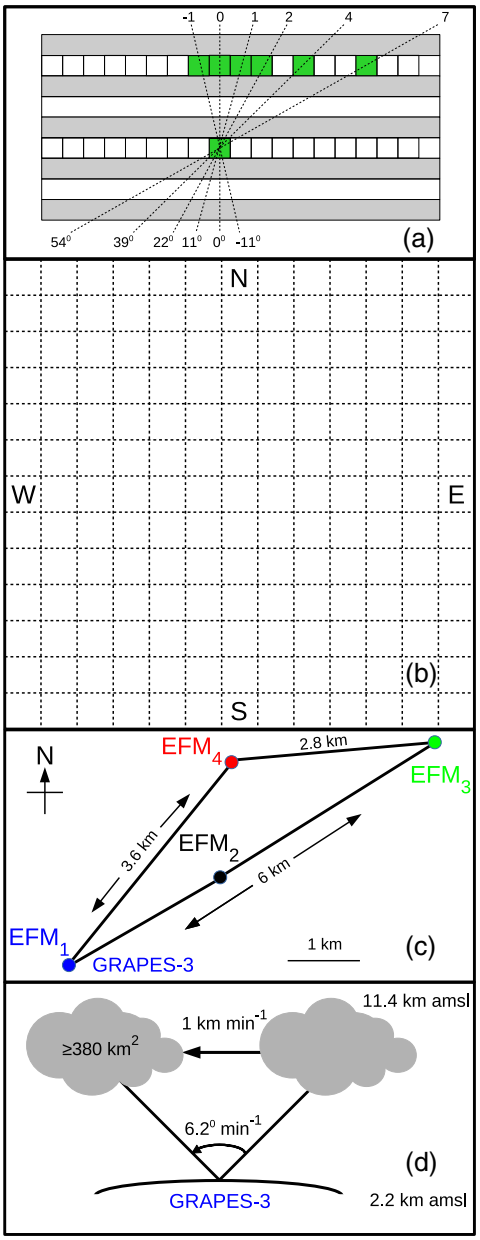


FIG. 1. (a) Reconstruction of muon directions in a single projection plane from PRC geometry, (b) telescope field of view (FOV) of 2.3 sr segmented into $13 \times 13 = 169$ directions, (c) locations of EFMs labeled 1 to 4. Maximum distance of $EFM_1$ and $EFM_3 = 6$ km, and (d) schematic of thundercloud movement (linear and angular velocities), altitude, and area.

The conversion of observed $\Delta I_\mu$ into equivalent potential $\mathbf{V}$ is derived from Monte Carlo simulations using the CORSIKA code [17] that, in turn, relies on the choice of hadronic interaction generators. Here, FLUKA [18] and SIBYLL [19] were used for the low- (<80 GeV) and high-energy (>80 GeV) interactions, respectively. When two

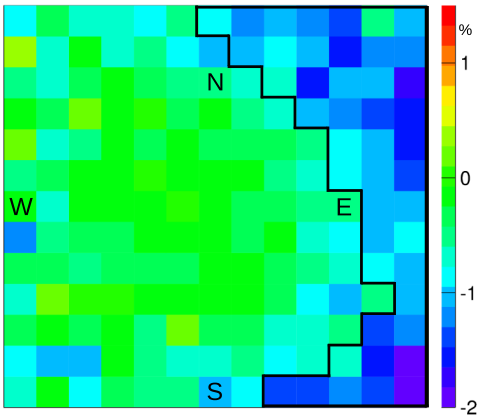


FIG. 2. Muon intensity variation during 18 min thunderstorm. Forty-five out of 169 thunderstorm affected contiguous directions are enclosed by the dark boundary. Color-coded percent variation shown by a bar on the right. Thundercloud angular size in N-S = 74.6°.

other popular high-energy generators (namely, QGSJET [20] or EPOS [21]) were used, an identical dependence of $\Delta I_\mu$ on $\mathbf{V}$ was obtained. This is because the affected muons are produced by low-energy (< 80 GeV) CRs where the high-energy generators are not used. But, when the other two low-energy generators, GHEISHA [22] or URQMD [23], were used, significant differences were observed. Compared to FLUKA, $\mathbf{V}$ inferred for GHEISHA was, on average, 15% higher; and for URQMD, it was 6% higher. FLUKA was chosen because it provided the lowest, and therefore the most conservative, estimate of the thundercloud potential. Next, the Monte Carlo simulation of muons detected by the G3MT in each of the 169 directions were carried out: first, with $\mathbf{V} = 0$; and then, by applying a $\mathbf{V}$ in the range of −3 to 3 GV in 0.1 GV steps over a height from 8 to 10 km amsl, as explained above. For each direction, the number of muons above the corresponding threshold energy was calculated. A high-statistics muon database of $10^7$ for $\mathbf{V} = 0$ and $10^6$ muons for each nonzero $\mathbf{V}$ was created. This allowed the simulated $\Delta I_\mu$ to be measured to 0.1% accuracy, which was much smaller than the error of 0.4–2.7% in real data.

The solar wind introduces a diurnal variation in $I_\mu$ that was removed by modeling with a higher-order polynomial after excluding thunderstorm affected 18 min data. The change in $I_\mu$ during 18 min is shown in Fig. 2. A cluster of 45 contiguous directions enclosed by a dark boundary displays a peak decrease of 2% ($20\sigma$ significance) in $I_\mu$, as shown in Fig. 3. During 10:42-10:59 UT, a clear decrease is visible to the right of the dark boundary in Fig. 2.

The simulated dependence of $I_\mu$ for 45 directions on applied potential $\mathbf{V}$ is shown in Fig. 4. A positive $\mathbf{V}$ at the thundercloud top relative to the bottom would lead to energy-loss of eV for $\mu^+$ and the same gain for $\mu^-$. Because of the ratio $\mu^+/\mu^- > 1.0$, the loss of detected $\mu^+$ exceeds the gain of $\mu^-$. Thus, the sum of muons of both polarities

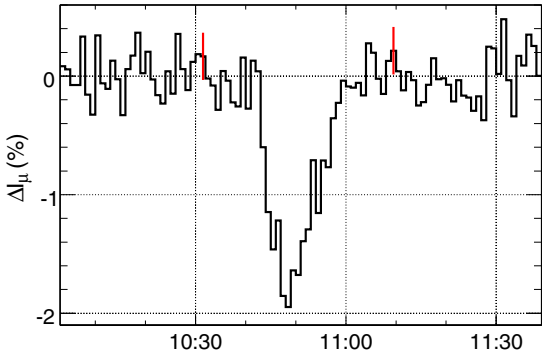


FIG. 3. Maximum muon intensity variation $\Delta I_\mu = -2\%$, starting at 10:42 Universal Time (UT) and lasting 18 min, seen during thunderstorm of December 1, 2014. Vertical bars represent $\pm 1\sigma$ error.

decreases for positive $\mathbf{V}$ and, beyond 1 GV, the slope gradually increases due to the rapid increase in decay probability of $\mu^+$, as seen in Fig. 4. This dependence is used to convert the measured $\Delta I_\mu$ into equivalent $\mathbf{V}$ that peaks at $(0.90 \pm 0.08)$ GV, as shown in Fig. 5.

The EFM records of the electric field (sample rate = 20 $s^{-1}$) show a smooth profile with rms = 0.01 kV $m^{-1}$ in all four cases, which is same as the EFM resolution. This suggests the absence of major lightning. Hereafter, the mean electric field ($min^{-1}$) is used for comparison with muon data ($min^{-1}$). Because all EFM profiles were similar and their amplitudes varied 22% around a mean of 3.3 kV $m^{-1}$, they were normalized to 3 kV $m^{-1}$, as shown in Fig. 6. $EFM_3$, after a delay of 4 min, was followed by $EFM_2$ and $EFM_4$: both of which overlapped. $EFM_1$, which was closest to the G3MT, was delayed by 6 min relative to $EFM_3$, indicating a thundercloud velocity of ∼1 km $min^{-1}$, moving from $EFM_3$ toward $EFM_1$, as shown schematically in Fig. 1(d).

Thundercloud movement in the FOV may be studied by the displacement of its muon image ($\Delta I_\mu$) in short 2 min exposures. Because short exposures reduce muon statistics thus, regions that showed ($I_\mu$) decrease in (a) contiguous directions or (b) isolated directions over ≥2 successive

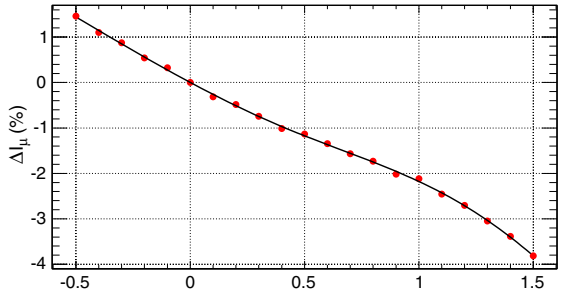


FIG. 4. Dependence of $\Delta I_\mu$ on electric potential (in gigavolts) across atmospheric layer of 8–10 km amsl, based on simulations for 45 directions shown in Fig. 2.

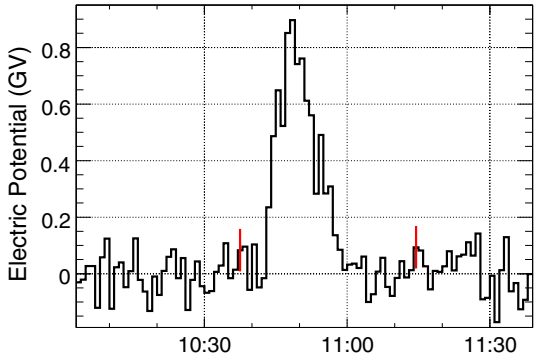


FIG. 5. Estimated electric potential shows a maximum of $(0.90 \pm 0.08)$ GV at 10:48 UT on December 1, 2014. Vertical bars represent $\pm 1\sigma$ error.

exposures were selected. In Fig. 7, $\Delta I_\mu$ for the first exposure starting at 10:42 UT is shown for the full FOV in the first top panel labeled **1**. A decrease in four directions enclosed by a dark boundary is visible, and the potential needed is shown in the bottom panel **1** of Fig. 7 that shows maximum $\mathbf{V} = 1.8$ GV during 10:41–11:00 UT. From the second panel onward, only 91 affected directions in the east are displayed. In the top panel labeled **2**, 12 affected directions require maximum $\mathbf{V} = 1.4$ GV. This decreases to 1 GV for panels labeled **3** (23) and **4** (32). Then, it increases to 1.1 and 1.2 GV for panels labeled **5** (28) and **6** (23), respectively. Finally, it reaches 1.4 GV for panels labeled **7** (16) and **8** (13). Integer values in the parentheses next to each panel number indicate the number of affected directions, which are highlighted by the dark boundaries in the corresponding top panels.

Successive panels in Fig. 7 show the western boundary of the muon image moving from east to west in the northern FOV. For example, it moved from direction **A** in the top panel labeled **1** to **B** in the top panel labeled **4** in 6 min, implying an angular velocity of 6.2° min$^{-1}$, as depicted in Fig. 1(d). A movement of 6.2° min$^{-1}$ of the muon image is seen in the southern FOV from **C** to **D** in the top panels labeled **3** and **6**, respectively. A similar movement is also reflected in the progressive shift of the peak voltage in the eight bottom panels of Fig. 7. If this angular velocity (6.2° min$^{-1}$) is combined with the linear velocity (1 km min$^{-1}$) from the EFMs, then a height of 11.4 km amsl is obtained, which is comparable to a typical thundercloud height (12 km) [3]. The 1 km min$^{-1}$ velocity and 11.4 km height are consistent with the velocity and height of a subtropical jet stream in south India [24].

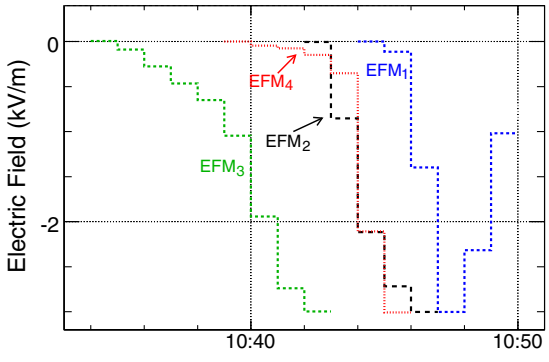


FIG. 6. $EFM_3$ profile appears first, followed by $EFM_2$ and $EFM_4$ after a 4 min delay. $EFM_1$ comes last, 6 min after $EFM_3$. Based on these EFM delays and locations from Fig. 1(c), a thundercloud velocity of 1 km min$^{-1}$ from east to west, shown schematically in Fig. 1(d), is inferred.

In north-south direction, the muon image covers the full FOV that corresponds to an angular size of 74.6°, as seen in Fig. 2. This implies a radius of $\geq 11$ km, which is very similar to average thundercloud radius (~12 km) [25] and yields a total area of this thundercloud of $\geq 380$ km$^2$. A thundercloud with infinitesimally thin charged regions, separated by 2 km, acts as a parallel-plate capacitor of a capacitance of $\geq 1.7$ $\mu$F. But, in reality, the thickness of the charged regions is comparable to their separation that reduces capacitance by ~50% to $\geq 0.85$ $\mu$F. $\mathbf{V} =$ 1.3 GV would require a total charge of $Q \geq 1100$ C and energy of $\geq 720$ GJ stored in this thundercloud. A 1.3 GV potential across the thundercloud with its two charged regions with a thickness 2 km each and a distance of 2 km between them implies an average field of 2.2 kV cm$^{-1}$, which is lower than the breakdown field at high altitudes [3]. The mean time to reach the maximum potential shown in the eight bottom panels in Fig. 7 is 6 min. Thus, the thundercloud would have delivered a power of $\geq 2$ GW, which is comparable to the single biggest nuclear reactors [26], as well as hydroelectric and thermal power generators [27]. The separation of 2 km used is reasonable because it extends the thundercloud top into the tropopause that defines the limit of cumulonimbus clouds producing major thunderstorms in the atmosphere [3]. Because the capacitance, total charge, energy stored, and power delivered by a thundercloud vary inversely with the separation of its charged layers, these parameters can be easily calculated for any other separation.

The potential can be measured by integrating the electric field over the thundercloud height. However, in general, the field measured by instruments aboard aircraft and balloons spans a region much smaller than the thundercloud height, and therefore cannot provide a reliable estimate of the potential. On the other hand, the parameter $\Delta I_\mu$ depends on the thundercloud potential and is virtually independent of its electric field and-or height. This makes muon telescopes with a giga-electron-volt threshold such as the G3MT ideal for measuring gigavolt potentials in thunderclouds. However, such high potentials cannot be indefinitely sustained, and a breakdown of air would result in acceleration of electrons to giga-electron-volt energies. It is conceivable that bremsstrahlung emission from giga-electron-volt electrons could produce photons ranging from

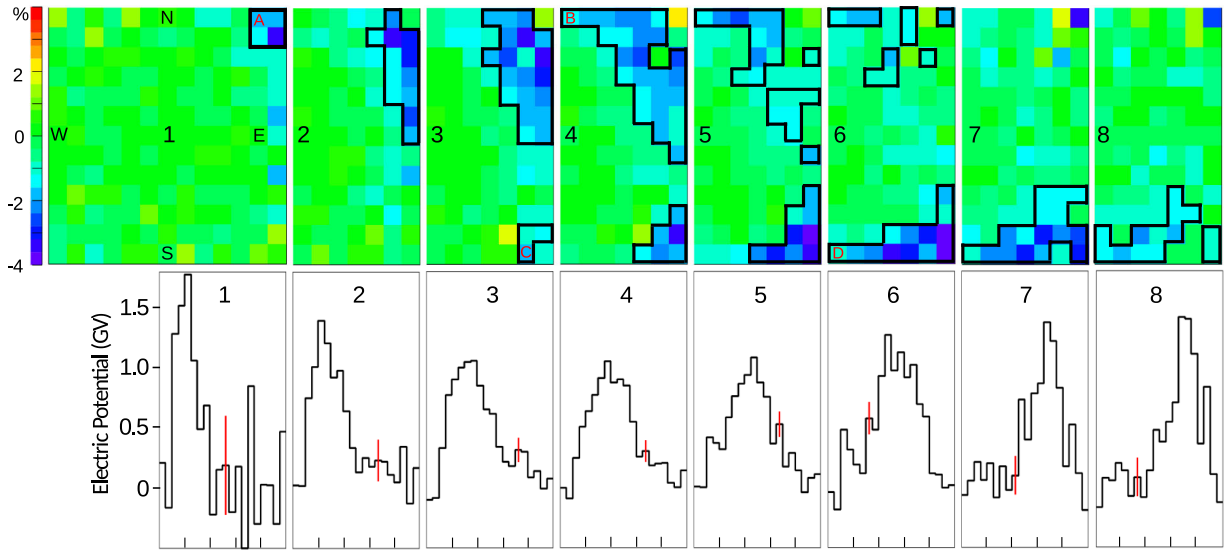


FIG. 7. Top eight panels show affected directions for successive 2 min exposures starting December 1, 2014 at 10:42 UT. Bottom eight panels show estimated potentials needed to reproduce $\Delta I_\mu$ shown in the corresponding panel above for a 20 min duration (10:41–11:00 UT). Maximum potentials of 1.8, 1.4, 1, 1, 1.1, 1.2, 1.3, and 1.4 GV (mean = 1.3 GV) observed for panels labeled 1 through 8. Angular velocity of 6.2° $\text{min}^{-1}$ inferred for directions (i) **A** to **B**, and (ii) **C** to **D** in northern and southern FOVs, respectively, are shown in Fig. 1(d). Vertical bar in each bottom panel corresponds to $\pm 1\sigma$ error.

a few to beyond 100 MeV in a short flash of terrestrial gamma rays.

*Conclusions.*—The GRAPES-3 muon telescope is well suited to measure the electric potential developed in thunderclouds, as shown for the December 1, 2014 event in which a peak electric potential of 1.3 GV was measured. This value is an order of magnitude larger than the previously reported maximum of 0.13 GV. This is possibly the first direct evidence for the generation of gigavolt potentials in thunderclouds, which is consistent with the prediction of Wilson 90 years ago [2]. The existence of gigavolt potentials could explain the production of highest-energy gamma rays in terrestrial gamma-ray flashes discovered 25 years back [4]. It is shown that $\geq 2$ GW of power, which are comparable to the single biggest nuclear reactors [26], as well as hydroelectric and thermal power generators [27], were delivered by this thunderstorm that was estimated to be moving at a speed of 60 $\text{km h}^{-1}$ near the top of the troposphere. Despite a simplified structure of the thundercloud used here, the present work provides reasonable insights into the physical state of the thunderstorms.

D. B. Arjunan, V. Jeyakumar, S. Kingston, K. Manjunath, S. Murugapandian, S. Pandurangan, B. Rajesh, K. Ramadass, V. Santhoshkumar, M. S. Shareef, C. Shobana, and R. Sureshkumar are thanked for assistance in running the GRAPES-3 experiment. The GRAPES-3 experiment was built with the generous support of TIFR and the Department of Atomic Energy, of the Government of India. This work was partially supported by grants from ISEE, Nagoya University, Chubu University, and the Ministry of Education and Science, Japan. We thank the three anonymous referees whose prompt, critical, and constructive comments led to a significant improvement in the final Letter and its early publication.

*gupta.crl@gmail.com

[1] B. Franklin, *Experiments and Observations on Electricity Made at Philadelphia in America* (E. Cave at St. John's Gate, London, 1751); Phil. Trans. R. Soc. London **47**, 565 (1752).
[2] C. T. R. Wilson, Nucl. J. Franklin Inst. **208**, 1 (1929); Proc. Phys. Soc. London **37**, 32D (1924); Proc. R. Soc. A **236**, 297 (1956).
[3] B. J. Mason, Proc. R. Soc. A **327**, 433 (1972); **415**, 303 (1988); J. Mason and N. Mason, Eur. J. Phys. **24**, S99 (2003); E. R. Williams, Sci. Am. **259**, No. 1–4, 88 (1988); C. P. R. Saunders, Space Sci. Rev. **137**, 335 (2008).
[4] G. J. Fishman *et al.*, Science **264**, 1313 (1994).
[5] M. Tavani *et al.*, Phys. Rev. Lett. **106**, 018501 (2011).
[6] T. C. Marshall and M. Stolzenburg, J. Geophys. Res. **106**, 4757 (2001).
[7] J. R. Dwyer *et al.*, Science **299**, 694 (2003).
[8] R. Ringuette, G. L. Case, M. L. Cherry, D. Granger, T. Gregory Guzik, M. Stewart, and J. P. Wefel, J. Geophys. Res. **118**, 7841 (2013).
[9] V. V. Alexeenko *et al.*, in *Proceedings of the 20th International Cosmic Ray Conference* (1987), Vol. 4, p. 272, http://adsabs.harvard.edu/abs/1987ICRC....4..272A.
[10] L. I. Dorman, I. V. Dorman, N. Iucci, M. Parisi, Y. Ne'eman, L. A. Pustil'nik, F. Signoretti, A. Sternlieb, G. Villoresi, and I. G. Zukerman, J. Geophys. Res. **108**, 1181 (2003).
[11] Y. Muraki, W. I. Axford, Y. Matsubara, K. Masuda, Y. Miyamoto, H. Menjyou, S. Sakakibara, T. Sako, T. Takami,

T. Yamada, S. Shibata, Y. Munakata, K. Munakata, S. Yasue, T. Sakai, K. Mitsui, K. Fujimoto, and E. Flückiger, Phys. Rev. D **69**, 123010 (2004).

[12] A. Chilingarian, S. Chilingaryan, T. Karapetyan, L. Kozliner, Y. Khanikyants, G. Hovsepyan, D. Pokhsraryan, and S. Soghomonyan, Sci. Rep. **7**, 1371 (2017).

[13] B. Hariharan *et al.*, Proc. Sci., ICRC2017 (**2017**) 481.

[14] S. K. Gupta *et al.*, Nucl. Instrum. Methods Phys. Res., Sect. A **540**, 311 (2005); Y. Hayashi *et al.*, Nucl. Instrum. Methods Phys. Res., Sect. A **545**, 643 (2005).

[15] P. K. Mohanty, K. P. Arunbabu, T. Aziz, S. R. Dugad, S. K. Gupta, B. Hariharan, P. Jagadeesan, A. Jain, S. D. Morris, B. S. Rao, Y. Hayashi, S. Kawakami, A. Oshima, S. Shibata, S. Raha, P. Subramanian, and H. Kojima, Phys. Rev. Lett. **117**, 171101 (2016); Phys. Rev. D **97**, 082001 (2018).

[16] https://www.boltek.com/product/efm100c-electric-eld-mill-kit.

[17] https://www.ikp.kit.edu/corsika.

[18] T. T. Bhlen, F. Cerutti, M. P. W. Chin, A. Fass, A. Ferrari, P. G. Ortega, A. Mairani, P. R. Sala, G. Smirnov, and V. Vlachoudis, Nucl. Data Sheets **120**, 211 (2014).

[19] E. J. Ahn, R. Engel, T. K. Gaisser, P. Lipari, and T. Stanev, Phys. Rev. D **80**, 094003 (2009).

[20] N. N. Kalmykov, S. S. Ostapchenko, and A. I. Pavlov, Nucl. Phys. B, Proc. Suppl. **52B**, 17 (1997).

[21] T. Pierog, I. Karpenko, J. M. Katzy, E. Yatsenko, and K. Werner, Phys. Rev. C **92**, 034906 (2015).

[22] http://cds.cern.ch/record/162911/files/CM-P00055931.pdf.

[23] http://urqmd.org.

[24] https://www.britannica.com/science/subtropical-jet-stream.

[25] http://www.nssl.noaa.gov/primer/tstorm/tst_basics.html.

[26] I. Pioro and R. Duffey, ASME J. of Nuclear Rad. Sci. **1**, 011001 (2015).

[27] https://www.power-technology.com/features/feature-the-10-biggest-hydroelectric-power-plants-in-the-world; https://www.power-technology.com/features/feature-giga-projects-the-worlds-biggest-thermal-power-plants.